Properties of wear-resistant WC-10Co-4Cr coatings prepared by high velocity oxy-fuel thermal spraying

Tran Phuong Chien, Nguyen Van Dung, Nguyen Hoang Duc, Nguyen Trong Cuong*

Institute for Tropical Technology (VITTEP), Academy of Military Science and Technology, 57A Truong Quoc Dung, Phu Nhuan, Ho Chi Minh City, Vietnam.
*Corresponding author: nguyencuongdbnd@gmail.com
Received 04 Jun. 2026; Revised 18 Aug. 2026; Accepted 04 Sep. 2026; Published 16 Sep. 2026.
DOI: https://doi.org/10.54939/1859-1043.j.mst.FMC.2026.45-52

ABSTRACT

This study aims to investigate and evaluate the microstructural characteristics, microhardness, and porosity of wear-resistant WC-10Co-4Cr cermet coatings deposited by high-velocity oxy-fuel (HVOF) thermal spraying. The methodology involves analyzing the morphological evolution of commercial cermet feedstock powder (with a particle size range of 15 – 45 µm) before and after interacting with the combustion gas stream (oxygen/propane) using scanning electron microscopy (SEM). The interface structure between the coating and the steel substrate, as well as the correlation between coating thickness and microhardness, were also investigated. The results indicate that under the high-temperature and supersonic velocity conditions of the HVOF spraying process, the initially porous cermet powder underwent surface densification. Concurrently, fine particle fragmentation occurred, leading to a decarburization reaction and the formation of the W_2C phase, a trend that significantly intensified at an oxygen/propane ratio of 300/55. At the interfacial boundary, the coating exhibited strong and sustainable bonding with the steel substrate. The coatings achieved excellent densification, with the porosity maintained at a very low level of 1% to 2%. The average microhardness of the entire specimen reached a high value of 628.86 HV, an adhesion strength of 63.2 MPa and a sliding wear rate of 1,65 x 10^{-5} mm^3/N.m for the sample with the highest hardness.

Keywords: WC-10Co-4Cr; HVOF.

1. INTRODUCTION

In the context of the continuous development in heavy industries such as oil and gas, marine, mining, and military, enhancing the service life of mechanical components operating under harsh working conditions has become an urgent necessity. Surface wear and corrosion are the two primary causes of severe degradation, which reduces operational efficiency and increases equipment maintenance costs. To address this issue, high-velocity oxy-fuel (HVOF) thermal spraying is one of the advanced and effective solutions for fabricating highly wear-resistant coatings [1]. Among the various thermal spray materials, the WC-10Co-4Cr cermet alloy has attracted significant attention due to its optimized composite structure: the ultra-hard tungsten carbide (WC) particles act as a reinforcing phase to resist wear, embedded within a tough Co-Cr binder matrix that effectively enhances both wear and corrosion resistance.

Currently, there is a tremendous demand within military maintenance and repair units for extending the service life of engine crankshafts in military hardware, such as tanks and armored vehicles. This study focuses on investigating and evaluating the microstructural characteristics, hardness, and porosity of WC-10Co-4Cr cermet coatings deposited via HVOF spraying technology. The obtained results will provide a reliable scientific database regarding the properties of protective material layers for crankshaft components, establishing a foundation to orient and master the thermal spray process guidelines, thereby ensuring the combat readiness of military hardware.

2. EXPERIMENT

2.1. Experimental material

The substrate material utilized was SCr440 steel with dimensions of 150 mm × 200 mm × 3 mm. This steel grade is widely employed for components operating in harsh environments subjected to friction, wear, and erosion. Prior to the thermal spraying process, the substrate surface was thoroughly cleaned and roughened.

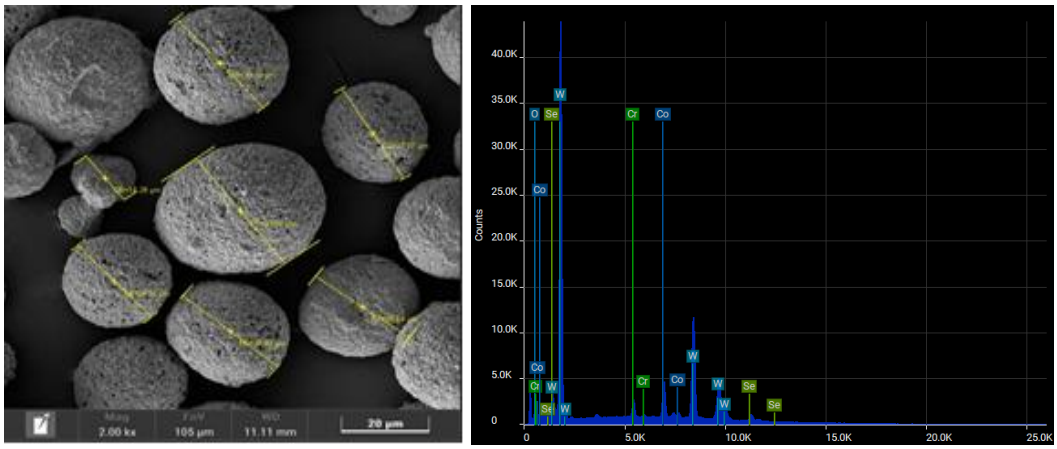


Figure 1. *SEM image and EDS analysis of the WC-10Co-4Cr thermal spray powder.*

The thermal spray powder selected for this study was WC-10Co-4Cr, supplied by AMST (India). The morphology and elemental composition of the feedstock powder were analyzed, as shown in Figure 1. The results indicate that the powder particles are spherical and well-separated, with a particle size range of approximately 15 – 40 μm. This represents a typical morphological feature of powders fabricated via the agglomerated and sintered method, where the particle surfaces exhibit high roughness and a characteristic porous structure with numerous micro-pores dispersedly distributed. This porous structure, formed by the evaporation of organic binders during the spray-drying and pre-sintering stages, increases the effective surface area. Consequently, it allows the powder particles to absorb thermal energy from the flame and accelerate more efficiently within the supersonic gas stream, thereby promoting a uniform semi-molten state prior to impacting the substrate surface.

EDS analysis also clearly confirms the presence of tungsten, cobalt, and chromium elements within the feedstock powder, as shown in Figure 1.

2.2. Spraying equipment and process

The equipment used was a Machjet 1 handheld HVOF spraying system, manufactured by AMST (India), as shown in Figure 2.

The quality of the HVOF-deposited coating highly depends on the technological parameters during the spraying process, particularly the combustion gas stream. The oxygen/propane (O_2/C_3H_8) ratio is a decisive factor governing the flame temperature, particle velocity, and the chemical interaction between the material particles and the surrounding environment, thereby directly affecting the coating's porosity, hardness, and decarburization behavior. To optimize the process guidelines and enhance coating performance, the research group referred to the optimal oxygen/propane ratios from previous studies, which ranged from 4 to 6 times. Consequently, the propane flow rate was kept constant at 55 L/min, while the oxygen flow rate was varied at two levels: 250 L/min and 300 L/min [2].

2.3. Characterization and testing methods

The microstructure and composition of the coatings were evaluated using a field-emission

scanning electron microscope (FESEM, MIRA LMU, Tescan, Czech Republic).

The phase composition was determined using an X-ray diffractometer (XRD, Aeris Mineral Edition, Malvern Panalytical, Netherlands.

The adhesion (or cohesion) strength was determined following ASTM C633 “Standard Test Method for Adhesion or Cohesion Strength of Thermal Spray Coatings” by an Elcometer 510 Model S pull-off adhesion tester with a 10 mm dolly.

The Vickers hardness was determined using a test load of 5 kgf by AFFRI, Italia.

The porosity was determined in accordance with the military standard TCQS 548:2025/VKHCNQS, entitled 'Morphological characterization of porous materials using scanning electron microscopy by a Tescan MIRA LMU high-resolution analytical scanning electron microscope (FE-SEM).

Table 1. *Spraying parameters.*

No	Spraying Parameters	Value
1	Compressed air pressure	8 bar
2	Oxygen pressure	10 bar
	Oxygen flow rate	250 L/min and 300 L/min
3	Propane pressure	6 bar
	Propane flow rate	55 L/min
4	Nitrogen pressure	5 bar
5	Spray angle	90^0
6	Spray distance	20 cm



Figure 2. *Machjet-1 HVOF spraying system.*

3. RESULTS AND DISCUSSION

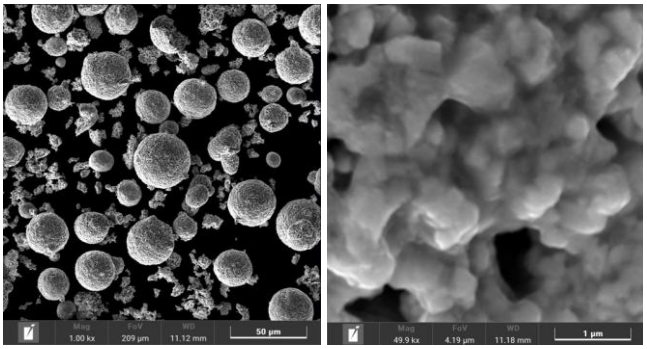
3.1. Characteristics of particles passing through the combustion gas stream

Figure 3 illustrates the surface morphology of the powder particles after exiting the combustion gas stream. The results indicate that the thermal interaction led to profound changes in the microstructure and phase transformation mechanisms. Although the particles retained their spherical geometry, their surfaces became noticeably smoother and denser. This demonstrates that under the extreme temperatures of the HVOF flame, the Co-Cr matrix phase underwent complete or partial melting, subsequently contracting due to surface tension and tightly encapsulating the unmelted WC carbide particles within.

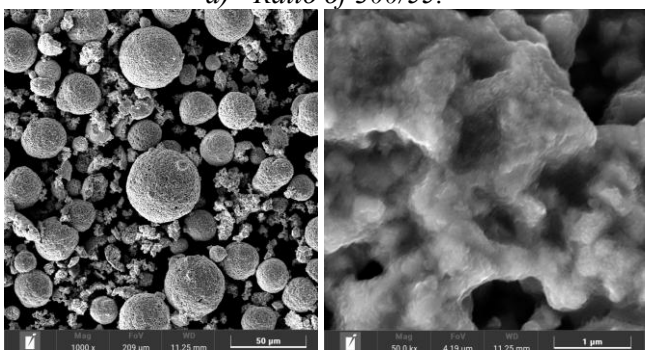
In addition to the large spherical particles, a significant amount of alternative fine fragments and irregularly shaped particles were found scattered throughout. This phenomenon is attributed to two primary mechanisms driven by the supersonic pressure and velocity of the gas stream. First, intrinsic thermal stress plays a key role: the extreme temperature gradient between the core and the shell of the cermet particles upon entering the flame induces thermal shock, causing the fragmentation of weakly bonded powder particles. Second, due to aerodynamic shearing, the ultra-high velocity of the supersonic combustion gas stream exerts a massive shear force on the molten matrix droplets, tearing away portions of the matrix along with small WC particles from the original spherical structure.

To evaluate the phase composition, X-ray diffraction (XRD) analysis was performed, as shown in Figure 4. The results indicate that after spraying at both oxygen flow rates, the powder passing

through the flame retained its primary WC phase. The cobalt and chromium peaks became weaker, which is consistent with the SEM observations. Concurrently, characteristic W_2C diffraction peaks appeared [3], with higher intensity observed at the flow rate of 300 L/min. This phenomenon can be explained by the increase in oxygen flow rate at the same propane fuel level, which led to a more complete combustion process and elevated the HVOF flame temperature. The excess heat from the flame caused overheating of the cermet particles during flight, promoting the thermal decomposition and dissolution of the tungsten carbide (WC) phase into W_2C. Additionally, the excess oxygen at the 300/55 ratio created a highly oxidizing environment, accelerating the decarburization of the WC phase and subsequently leading to a higher phase density accumulation of W_2C within the coating structure [4].



a) Ratio of 300/55.



b) Ratio of 250/55.

Figure 3. *SEM morphology of powder particles after passing through the combustion gas stream.*

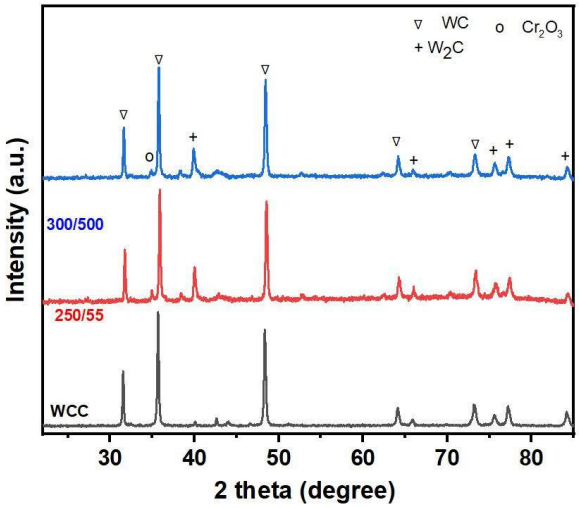


Figure 4. *XRD pattern of thermal-treated and initial powder.*

Elemental composition and distribution ratios were analyzed as presented in Table 2. The energy-dispersive X-ray spectroscopy (EDS) results reveal a distinct shift in the content and distribution of the baseline elements (W, Co, Cr) within the surveyed area upon altering the technological parameters.

Specifically, at the 300/55 gas flow ratio, the density of these elements was significantly higher than that observed at the 250/55 ratio. This increase in the concentrations of W, Cr, and Co within the splat structure is directly correlated with the kinetics of the HVOF spraying process. At the higher energy ratio (300/55), the sharply elevated temperature and velocity of the gas stream promoted the thorough melting of the Co-Cr binder matrix. This facilitated enhanced adhesion of the alloying elements and a uniform dispersion around the carbide particles. The high W content (derived from the partial dissolution of the hard particles) synergistically combined with Cr in the Co matrix. This not only enhances the phase bond strength through the solid-solution strengthening mechanism but also establishes a precursor for the formation of Cr- and W-rich protective oxide films during friction. This positive evolution in elemental composition at the 300/55 ratio serves as the key factor in improving the microhardness and optimizing the wear resistance of the WC-10Co-4Cr coating. Consequently, the 300/55 ratio was selected for the subsequent deposition of the coatings onto the steel substrates.

Table 2. *Molar composition of powder particles after thermal interaction.*

250/55						300/55					
Mapping	W (%)	C (%)	Co (%)	Cr (%)	O (%)	Mapping	W (%)	C (%)	Co (%)	Cr (%)	O (%)
1	11.00	71.88	6.01	3.40	7.70	1	11.07	67.99	5.22	2.87	12.84
2	9.90	70.86	5.87	2.59	7.91	2	14.56	69.13	6.43	3.23	6.66
3	5.91	83.31	3.01	1.47	6.29	3	7.99	76.55	3.69	1.96	9.81
4	9.09	77.07	4.30	2.30	7.23	4	9.56	71.89	5.48	2.84	10.23
5	10.47	72.60	5.08	2.82	9.03	5	8.85	74.94	4.38	2.32	9.51
6	7.74	75.54	3.25	1.66	11.80	6	10.74	66.67	5.53	2.74	10.65
						7	11.93	70.49	5.57	3.28	8.74
Average	9.02	75.21	4.58	2.37	8.33	Average	10.67	71.09	5.18	2.74	9.77

3.2. Properties of the coatings on steel substrates

The WC-10Co-4Cr powder was deposited onto the steel substrates at an oxygen/propane flow ratio of 300/55. The SEM analysis results, as presented in Figure 5, reveal that the interface between the coating (upper bright region) and the steel substrate (lower dark region) exhibits a wavy and non-linear morphology. This characteristic demonstrates that the surface of the steel substrate had undergone effective mechanical grit-blasting treatment prior to spraying.

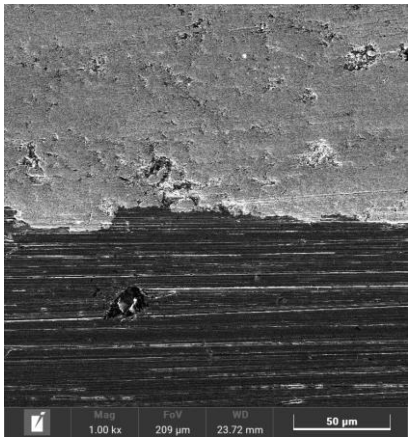


Figure 5. *Cross-sectional SEM morphology of the coating/substrate interface.*

The upper coating exhibits a highly dense structure with a uniform distribution of carbide particles. Near the interface, the coating is virtually free of cracks or delamination, demonstrating the uniformity of dynamic pressure as successive splats flatten onto one another. This indicates that the in-flight particles, passing through the combustion gas stream in a semi-molten state, impacted the roughened surface at supersonic velocities. Consequently, they underwent intense plastic deformation, filling the roughness valleys and tightly gripping the roughness peaks of the steel substrate. However, a few localized micro-voids can still be observed within the coating or along the interface. This phenomenon is attributed to the extremely rapid cooling of the molten droplets upon hitting the cold steel substrate, which prevented the material flow from completely filling the deepest roughness recesses, or to the adherence of early-cooled rebound particles. Nevertheless, the fraction of these pores remains negligible and discontinuous, thereby ensuring high structural integrity for the coated component.

Furthermore, porosity analysis reveals that the coating possesses a highly dense structure, with the porosity retained at a very low level, ranging only between 1–2%, consistent with other studies [5, 6]. This indicates that under the supersonic pressure and velocity of the combustion gas stream, the in-flight particles impact the substrate surface with immense kinetic energy. This high inertial force flattens the molten droplets into tightly stacked splat structures, eliminating most of the intra-particle and inter-particle air voids, thereby enhancing the physicomechanical properties of the coating. The low porosity minimizes stress concentration points, preventing the initiation and propagation of micro-cracks under external mechanical loads. Concurrently, this dense structure acts as an effective barrier, impeding corrosive agents from penetrating through the coating to reach the steel substrate, thus ensuring superior wear resistance and corrosion protection for the component under real working conditions [7].

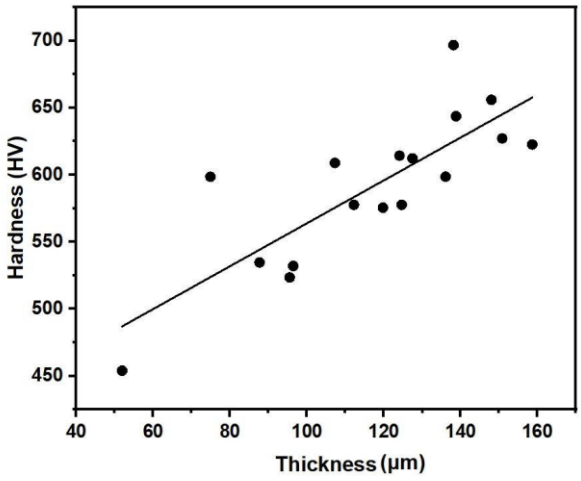


Figure 6. *Correlation between coating thickness and hardness.*

Analysis of the coating hardness and thickness, as shown in Figure 6, reveals a clear directly proportional relationship: the microhardness tends to increase gradually and stabilize as the coating thickness rises from approximately 51.9 μm to nearly 160 μm. In the lower thickness ranges (≤ 100 μm), the hardness values exhibit a wide dispersion and are notably lower, fluctuating between 450 – 550 HV, which is still significantly higher than the substrate hardness of 143 HV. This phenomenon is attributed to the substrate effect. When the coating is too thin, it suffers from stress penetrating through the film layer and reaching the plastic deformation zone of the softer underlying steel substrate, thereby reducing the actual measured hardness value. As the coating thickness exceeds the 120 μm threshold, the hardness values become highly concentrated around 600 – 700 HV, reaching a local peak of approximately 700 HV at a thickness near 138 μm. At this

stage, the coating is thick enough to completely eliminate the substrate effect. This increase in hardness reflects the cumulative nature of the multi-pass spraying process. However, when the coating thickness exceeds 138 μm, the hardness tends to decrease. Continued increases in film thickness lead to a severe accumulation of intrinsic tensile residual stresses and an in-situ annealing effect. This phenomenon promotes the formation of micro-cracks at the splat boundaries and softens the Co-Cr binder matrix, resulting in a reversal effect: the coating porosity tends to increase and the microhardness begins to decline, which is consistent with several previous studies [8-9]. Concurrently, coating analysis revealed an adhesion strength of 63.2 MPa and a sliding wear rate of 1,65 x 10^{-5} mm^3/N.m for the sample with the highest hardness.

4. CONCLUSIONS

This study successfully fabricated high-quality WC-10Co-4Cr coatings using High-Velocity Oxygen-Fuel (HVOF) thermal spray technology and elucidated the material transformation mechanism from the initial porous powder to a highly dense structure upon interaction with the combustion gas stream. Experimental results demonstrate that although the oxygen/propane flow ratio of 300/55 induced the formation of the W_2C decarburization phase, it promoted the thorough semi-molten state of the binder matrix and enhanced the distribution density of the baseline elements (W, Co, Cr), thereby optimizing the wear resistance. The coating exhibited robust adhesion to the steel substrate, achieving a highly dense microstructure with a remarkably low porosity maintained between 1% and 2%. Notably, the average microhardness of the entire specimen reached an impressive value of 628,86 HV, an adhesion strength of 63.2 MPa and a sliding wear rate of 1,65 x 10^{-5} mm^3/N.m for the sample with the highest hardness. These findings establish a solid precursor for applying HVOF thermal spray technology to components demanding superior wear and corrosion resistance in harsh operating environments—such as the crankshafts of armored tank engines—thereby contributing to extending their service life and ensuring the combat readiness of the military.

Acknowledgements: *The authors would like to acknowledge the financial support from the project titled 'Research on technologies and materials for WC-Co-Cr and YSZ ceramic thermal spray coatings applied to the restoration and fabrication of wear- and heat-resistant components in military technical equipment'. We also sincerely thank Assoc. Prof. Le Anh Kien for his valuable guidance and scientific insights.*

REFERENCES

[1]. Nguyễn Thanh Phú, *"Nghiên cứu ảnh hưởng của một số thông số công nghệ phun phủ HVOF đến chất lượng lớp phủ bề mặt chi tiết làm việc trong điều kiện khắc nghiệt bị mòn"*, Luận án Tiến sĩ Kỹ thuật Cơ khí, Viện Nghiên cứu Cơ khí, Hà Nội, (2020) (in Vietnamese).

[2]. Nguyễn Thanh Phú và cộng sự, *"Tối ưu hóa các thông số quá trình phun HVOF để nâng cao độ bám dính của lớp phủ WC-12Co Optimizing HVOF spray process parameters to improve adhesion of WC-12Co coatings"*, Hội nghị khoa học và công nghệ về cơ khí lần thứ V – VCME, (2018) (in Vietnamese).

[3]. Schlachta, Patrick, et al., *"Synthesis of Phase-Pure W2C and WC by Separation of Reduction and Carburization and Their Differing Performance as Hydrogenation Catalysts"*, The Journal of Physical Chemistry C 129.47, pp. 20907-20921, (2025).

[4]. Grabowski, Theresa, et al., *"Microstructural evaluation of tungsten carbide cobalt (WC-17Co) alloy deposited by high-velocity oxygen fuel, high-velocity air fuel, and cold spraying technologies"*, Journal of Thermal Spray Technology 33.2, pp. 719-731, (2024).

[5]. Shu, Wenxiang, et al., *"Microstructure and wear resistance of HVOF sprayed WC-10Co-4Cr coating on Ti-6Al-4V"*, Heat Treatment and Surface Engineering 4.1, pp. 70-75, (2022).

[6]. El Rayes, Magdy M., El-Sayed M. Sherif, and Hany S. Abdo, *"Comparative study into microstructural and mechanical characterization of HVOF-WC-based coatings"*, Crystals 12.7, p. 969, (2022).

[7]. Picas, Josep A., et al., *"Influence of HVOF spraying parameters on the corrosion resistance of WC–CoCr coatings in strong acidic environment"*, Surface and coatings technology 225, pp. 47-57, (2013).

[8]. Rajendran, Pradeep Raj, et al., *"Optimisation of HVOF spray process parameters to achieve minimum porosity and maximum hardness in WC-10Ni-5Cr coatings"*, Coatings 12.3, p. 339, (2022).
[9]. Murariu, Alin Constantin, and Ion Aurel Perianu, *"Influence of HVOF deposition thickness on adhesion strength of WC–CrC–Ni coatings"*, Advanced Technologies and Materials 44.1, pp. 33-40, (2019).

TÓM TẮT

Đặc tính lớp phủ hợp kim kháng mài mòn WC-10Co-4Cr bằng công nghệ phun phủ oxy nhiên liệu tốc độ cao

Nghiên cứu này nhằm mục đích khảo sát và đánh giá các đặc tính vi cấu trúc, độ cứng vi mô và độ xốp của lớp phủ hợp kim kháng mài mòn WC-10Co-4Cr chế tạo bằng công nghệ phun phủ nhiệt tốc độ cao (HVOF). Phương pháp nghiên cứu bao gồm việc phân tích sự biến đổi hình thái học của bột cermet thương mại (kích thước 15 – 45µm) trước và sau khi tương tác với dòng khí cháy (oxy/propan) thông qua hiển vi điện tử quét (SEM). Cấu trúc vùng biên giới tiếp xúc giữa lớp phủ và nền thép, cùng mối tương quan giữa độ dày và độ cứng vi mô cũng được tiến hành khảo sát. Kết quả nghiên cứu chỉ ra rằng dưới tác động nhiệt-tốc độ phun siêu thanh công nghệ phu phủ HVOF, bột cermet xốp ban đầu đã đặc chắc hóa bề mặt, đồng thời xảy ra hiện tượng phân tách hạt mịn dẫn đến phản ứng khử cacbit hình thành pha W_2C (xu hướng tăng mạnh ở tỷ lệ oxy/propan là 300/55. Tại vùng ranh giới tiếp xúc, lớp phủ đã bám chặt vào nền thép bền vững. Lớp phủ đạt độ đặc tốt, với tỷ lệ lỗ xốp duy trì ở mức rất thấp từ 1% đến 2%. Độ cứng vi mô trung bình của toàn mẫu đạt giá trị cao là 628,86 HV, độ bám dính đạt 63,2 Mpa và tốc độ mài mòn trượt đạt 1,65 x 10^{-5} mm^3/N.m ở mẫu có độ cứng cao nhất.

Keywords: WC-10Co-4Cr; HVOF.